

報告

Evaluation of Semiconductor Dosimeter for Measuring Air Kerma Including Scattered Radiation

Takeshi TAKAKI¹⁾, Ryohei KUROKI²⁾, Yuki FUJITA²⁾, Seiichi MURAKAMI¹⁾

- 1) Department of Radiological Science, Faculty of Health Sciences, JUNSHIN GAKUEN University
- 2) Department of Radiology, Hospital of University of Occupational and Environmental Health

Abstract: Although complex to handle, ionization chambers are standard instruments for radiation dosimetry. This study compared two semiconductor dosimeters (the Dose Probe and Piranha 657) with an ionization chamber to evaluate the accuracy of air kerma measurements, including scattered radiation. The dose, energy, and object thickness dependence were verified using PMMA. The relative dose and error were calculated using an ionization chamber as the reference. The results showed that the Dose Probe maintained relative errors below 5% in all tests, which closely matched those of the ionization chamber. This confirmed the ability of the Dose Probe to accurately measure the absorbed dose, including the scatter radiation, suggesting its practicality for clinical use. This study validated the use of semiconductor dosimeters in clinical settings, supporting a simplified setup, potentially improving the measurement accuracy near detectors and enhancing dose management in radiographic practice.

Key words: Semiconductor Dosimeter, Dose optimization, Air kerma, Scattered radiation, digital radiography

1. INTRODUCTION

As a standard measurement method for the absorbed dose in the diagnostic X-ray region, the effective energy is calculated from the half-value layer to obtain the incident air kerma, which is then converted into the incident surface air kerma by considering a backscatter factor¹. In air-kerma measurements, an ionization chamber is generally used as a reference dosimeter, considering characteristics such as low energy influence and direction dependence. However, ionization chambers have certain disadvantages. It is necessary to correct the temperature and atmospheric pressure, and it is frequently difficult to measure the dose under the geometric conditions desired by the user owing to the dosimeter's size and shape. Hamasaki et al. proved the usefulness of a semiconductor dosimeter using a noninvasive X-ray analyzer². A semiconductor dosimeter can measure a dose without correcting for temperature or atmospheric pressure. In addition, simple and compact products are sold and are easy to handle.

Most studies have determined the relationship between X-ray dose and image quality based on the

results of the dose area product, entrance skin dose (or entrance surface dose), or visual evaluation³⁻⁵. However, image quality is related to the incident dose on the detector, and it is important to evaluate the detector dose value. Although the exposure index can estimate the dose reaching the detector, it is dependent on the dose quality^{6,7}. Therefore, accurately simulating actual clinical conditions and conducting dose measurements at locations that reflect the geometric setup encountered in clinical practice is crucial. These considerations may contribute to improving image quality control in clinical practice. However, to the best of our knowledge, no study has compared and verified the air kerma after passing through an object. Ionization chambers are widely recognized as the gold standard for dose measurements, making them ideal benchmarks for verifying the accuracy of semiconductor dosimeters. Therefore, in this study, the dose, energy, and object thickness dependences after scattered penetration were evaluated using dose-probe semiconductor dosimeters with an ionization chamber as the reference dosimeter, and the accuracy of the semiconductor dosimeter was verified.

2. MATERIALS AND METHODS

2.1 Materials

A UD150B-40 was used as the X-ray generator (Shimadzu Corp., Kyoto, Japan). Twenty sheets of 10-mm-thick polymethyl methacrylate (PMMA) ($40 \times 30 \text{ cm}^2$) were used as the scatter material. The X-ray dose after passing through an object is defined as air kerma. For dose measurement, a farmer-type ionization chamber $10 \times 5\text{-}6$ (Radcal Corp., USA), dose monitor Model 9015 (Radcal Corp.), semiconductor Piranha 657, and Dose Probe (RTI Group AB, Sweden) were used. The Dose Probe is a semiconductor detector connected externally to a Piranha 657 semiconductor dosimeter. All dosimeters were calibrated. The appearance, dimensions, weight, and detector size of the dosimeters, that is, the ionization chamber, Dose Probe, and Piranha 657 are detailed in Fig. 1 and Table 1.

2.2 Geometry

The geometric conditions are shown in Fig. 2. The

source-to-dosimeter distance was set to 100 cm, and the semiconductor dosimeter was placed 100 cm from the source. Each dosimeter was placed at least 150 cm away from the wall to prevent backscattering from the room wall. The dosimeter was set 100 cm above the floor and placed on the rear surface of the PMMA for the X-ray beam. The ionization chamber and the semiconductor dosimeters were positioned with their measured surface centers aligned with the center of the radiation field. The field size was adjusted $10 \times 10 \text{ cm}^2$ in front of the PMMA surface. X-rays were irradiated parallel to the floor. Under these geometric conditions, the dose, energy, and object thickness dependences were evaluated using an ionization chamber, Piranha 657, and a Dose Probe.

2.3 Evaluation items

An ionization chamber was used as the reference dosimeter. The air kerma, energy, and object thickness dependences after scattered penetration were measured using an ionization chamber, Piranha 657, and a Dose

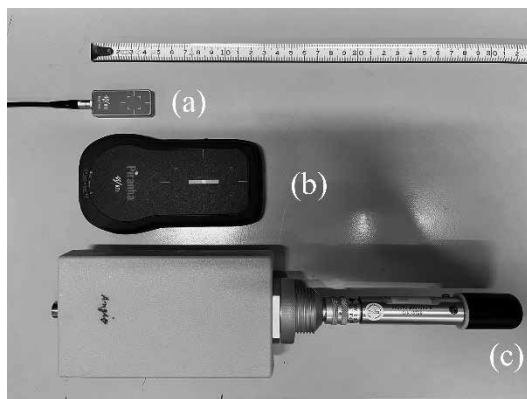


Figure 1. Semiconductor dosimeters with different shapes used. (a) Dose Probe, (b) Piranha 657, and (c) ionization chamber.

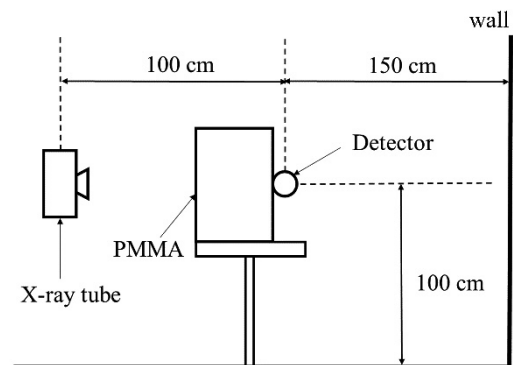


Figure 2. Geometrical conditions of measurements. Source-to-image detector distance was set to 100 cm. The ionization chamber and each semiconductor dosimeter were placed behind the PMMA to detect scattered radiation.

Table 1. Comparison of the features of semiconductor dosimeters and ionization chamber. The size and weight of the Dose Probe are lower than that of the Piranha 657 and ionization chamber. The detector area of the Dose Probe is greater than that of the Piranha 657 but lower than that of the ionization chamber.

| | Dose Probe | Piranha 657 | Ionization chamber |
|--------------------|-------------------------------|---------------------------------|---------------------------------|
| Size (mm) | $19.8 \times 45.0 \times 7.4$ | $133.0 \times 75.0 \times 26.0$ | $310.0 \times 80.0 \times 40.0$ |
| Weight (g) | 85 | 406 | 500 |
| Detector area (mm) | 10×10 | 2×2 | $25\phi \times 38$ |

Probe. The air-kerma measurement accuracies of the semiconductor dosimeters were verified by comparing their measured values with those of the ionization chamber. The ionization chamber, Piranha 657, and the Dose Probe were set up and measured separately. The air kerma in the ionization chamber was calculated using the following equation (1):

$$K_a = W_{air} \cdot M \cdot N \cdot k_{TP} \cdots (1)$$

where K_a is the air kerma, W_{air} is the W value (33.97), M is the measured reading from the dosimeter, N is the dosimeter calibration factor, and k_{TP} is the temperature and pressure correction factor. Internal calibration of the device was used for the semiconductor dosimeter, which was automatically adjusted for different beam qualities based on the measured spectrum. The measurements were performed three times at all measurement points, and the average value was used as the value at each measurement point.

Additionally, the relative air kerma values of the ionization chamber and Dose Probe, as well as the relative error between the ionization chamber and the semiconductor dosimeter, were calculated using Equations 2 and 3.

$$Relative\ value = D_{semi} / D_{ion} \cdots (2)$$

$$Relative\ error = (D_{semi} - D_{ion}) / D_{ion} \times 100 \cdots (3)$$

where D_{ion} is the value of air kerma in the ionization chamber, and D_{semi} is the value of air kerma in the semiconductor dosimeter.

2.3.1 Dose dependence

Dose dependence was calculated using the following conditions: The PMMA thickness was 10 cm, the tube voltage was 80 kV, the tube current was 630 mA, and the tube current-time product (mAs) was changed to 2, 8, 16, 25, and 32. After passing through the object, the air kerma was measured using the previously described ionization chamber and two semiconductor dosimeters.

2.3.2 Energy dependence

To evaluate the energy dependence of the dosimeters, the air kerma was measured while varying

the X-ray beam energy by fixing the PMMA thickness to 10 cm, and the tube current-time product was set at 2 mAs. The tube voltage was then changed from 60 to 120 kV in 10 kV increments. This range of tube voltages covers the typical energies used in diagnostic radiography, allowing us to assess dosimeter performance across various clinical scenarios.

2.3.3 Object thickness dependence

To assess the object-thickness dependence of the dosimeters, the air kerma was measured while simulating patients of different body sizes. This approach allowed us to evaluate the dosimeter response characteristics under various scatter conditions and assess the clinical reproducibility. The tube voltage was fixed at 80 kV, the tube current-time product was set at 20 mAs, and the PMMA thickness was varied from 5 to 20 cm in 5 cm increments. This range of thickness represents variations in the body size from pediatric to adult patients, allowing us to evaluate how dosimeters perform across different patient body size.

3. RESULTS

3.1 Dose dependence

Table 2 lists the coefficients of variation for the ionization chamber and each semiconductor dosimeter at various mAs values. The ionization chamber dosimeter exhibited higher coefficients of variation than the two semiconductor dosimeters at low mAs values, indicating relatively large measurement uncertainties in the low-dose range. In contrast, the semiconductor detectors (Dose Probe and Piranha 657) maintained stable, low coefficients of variation across the entire mAs range. In the high-dose range, all detectors showed coefficients of variation below 0.002, confirming measurement stability at high doses.

Figure 3(a) shows the relative air kerma values of the ionization chamber and two semiconductor dosimeters when the tube current-time product was changed. Fig. 3(b) shows the relative error at each measurement point. The relative value of the Dose Probe was approximately 1 and that of Piranha 657

was approximately 0.5. The relative error of the Dose Probe at each point was within 5%; however, the Piranha 657 had a high relative error of $\leq 40\%$.

3. 2 Energy dependence

Table 3 lists the coefficients of variation of the ionization chamber and semiconductor dosimeters (Dose Probe and Piranha 657) at various kV values. The ionization chamber showed relatively high coefficients of variation at lower kV values (60-90 kV), with a decreasing trend as the kV increased. In contrast, semiconductor detectors maintain relatively stable and low coefficients of variation across the entire kilovoltage range. In the high-kilovoltage range (100-120 kV), all detectors exhibited coefficients of variation < 0.006 , confirming the measurement stability in the high-energy region.

Figure 4(a) shows the relative air kerma values of the ionization chamber and two semiconductor dosimeters when the tube voltage was changed. Fig. 4 (b) shows the relative error at each measurement point. The relative value of the Dose Probe was approximately 1 and that of Piranha 657 was approximately 0.5. The relative error of the Dose Probe at each point was within 5%, whereas the high relative error of the Piranha 657 was $> 40\%$.

3. 3 Object thickness dependence

Table 4 shows the coefficients of variation of the ionization chamber and semiconductor dosimeters (Dose Probe and Piranha 657) for various PMMA thicknesses. The ionization chamber maintains low coefficients of variation at smaller PMMA thicknesses (0-15 cm), but shows a sharp increase in variation at a thickness of 20 cm. In contrast, semiconductor

detectors demonstrated very stable and low coefficients of variation across the entire PMMA thickness range.

Figure 5(a) shows the relative air kerma values of the ionization chamber and two semiconductor dosimeters when the PMMA thickness was changed. Fig. 5(b) shows the relative error at each measurement point. The relative value when using the Dose Probe was approximately 1 and between 0.4 and 0.6 in the Piranha 657. The relative error of the Dose Probe at each point is within 5%. Conversely, for the Piranha 657, the relative error was $> 30\%$ and increased further as the PMMA thickness increased.

4. DISCUSSION

Although the ionization chamber showed slightly higher variability, especially at low mAs values and thick PMMA thicknesses, with CV values reaching 0.015 (1.5%), all the dosimeters demonstrated coefficients of variation values < 0.05 (5%). Similar to the results of Hamasaki et al., these results indicate excellent measurement reproducibility².

The accuracy of semiconductor dosimeters has been evaluated and compared with that of an ionization chamber for measuring air kerma⁸⁻¹⁰. However, the performance of dose probes for measuring air kerma, including scattered radiation, has not been examined extensively. Therefore, in this study, we compared the Dose Probe and Piranha 657 using an ionization chamber as the gold standard. Regarding dose and energy dependence, the accuracy was verified by changing the tube current-time product or tube voltage with an object of a certain thickness. As a result of this evaluation, the relative error between the ionization chamber and the Dose Probe was found to be within

Table 2. Comparison of coefficients of variation for the ionization chamber dosimeter and semiconductor dosimeters (Dose Probe and Piranha 657) at various mAs values.

| | Tube current-time product (mAs) | | | | |
|---------------------------|---------------------------------|-------|-------|-------|-------|
| | 2 | 8 | 16 | 24 | 32 |
| Ionization chamber | 0.012 | 0.005 | 0.002 | 0.000 | 0.001 |
| Dose Probe | 0.001 | 0.001 | 0.001 | 0.000 | 0.000 |
| Piranha 657 | 0.005 | 0.001 | 0.001 | 0.002 | 0.001 |

Table 3. Comparison of coefficients of variation for the ionization chamber dosimeter and semiconductor dosimeters (Dose Probe and Piranha 657) at various kV values.

| | kilovoltage range | | | | | | |
|---------------------------|-------------------|-------|-------|-------|-------|-------|-------|
| | 60 | 70 | 80 | 90 | 100 | 110 | 120 |
| Ionization chamber | 0.015 | 0.018 | 0.010 | 0.012 | 0.005 | 0.004 | 0.003 |
| Dose Probe | 0.005 | 0.003 | 0.002 | 0.001 | 0.006 | 0.004 | 0.003 |
| Piranha 657 | 0.003 | 0.003 | 0.005 | 0.004 | 0.002 | 0.002 | 0.005 |

Table 4. Comparison of coefficients of variation for the ionization chamber dosimeter and semiconductor dosimeters (Dose Probe and Piranha 657) at various PMMA thicknesses.

| | PMMA thickness (cm) | | | | |
|---------------------------|---------------------|-------|-------|-------|-------|
| | 0 | 5 | 10 | 15 | 20 |
| Ionization chamber | 0.001 | 0.001 | 0.003 | 0.003 | 0.012 |
| Dose Probe | 0.001 | 0.000 | 0.001 | 0.001 | 0.002 |
| Piranha 657 | 0.001 | 0.001 | 0.000 | 0.001 | 0.002 |

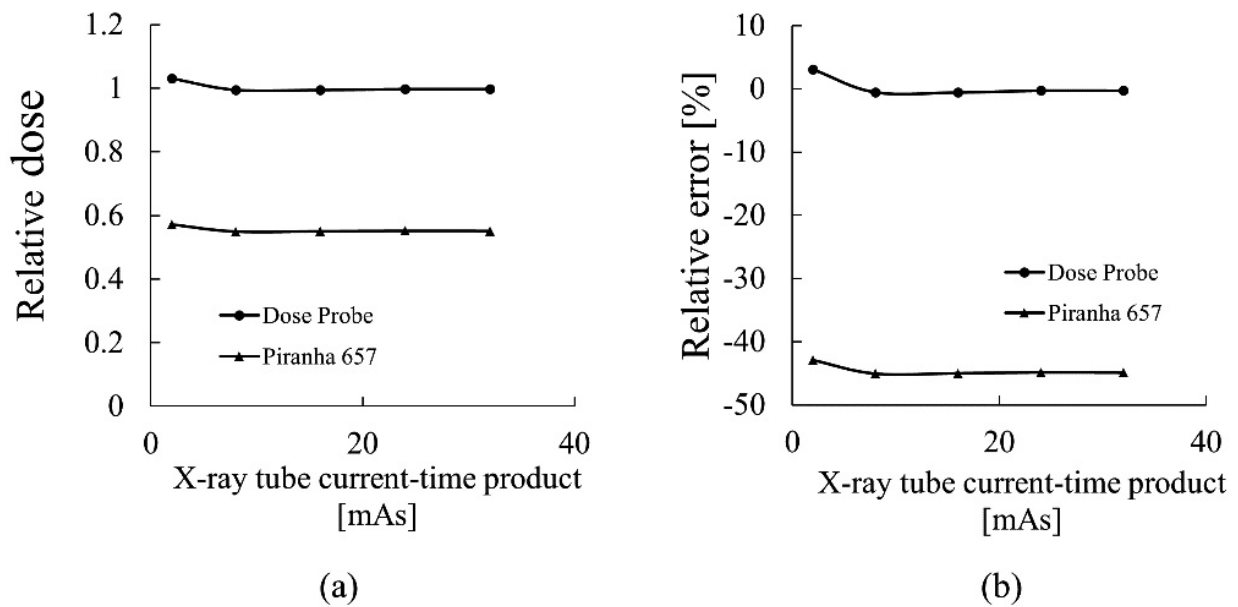


Figure 3. Ratio of the value of each semiconductor dosimeter with the value of the ionization chamber at dose dependence. The Ratio in the case of using the Dose Probe was approximately 1 compared to the Piranha 657. The ratios did not fluctuate when the mAs value was increased or decreased (a). The relative error was <5% when using the Dose Probe (b). In contrast, the relative error of the Piranha 657 was >40% (b).

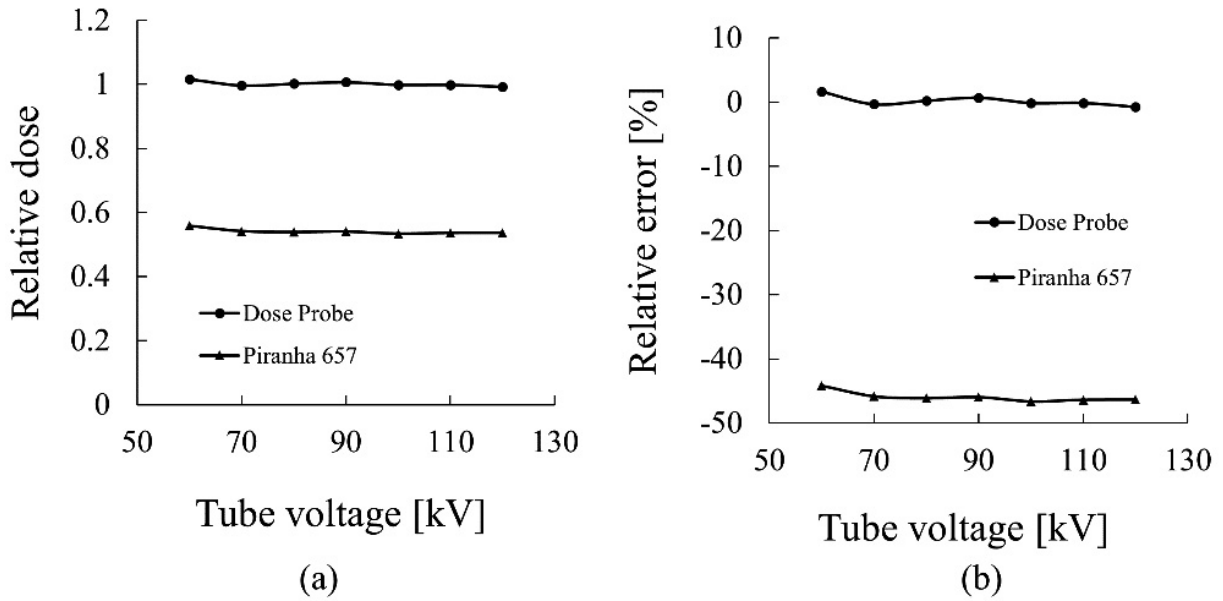


Figure 4. Ratio of the value of each semiconductor dosimeters with the value of the ion chamber at energy dependence. The Ratio in the case of using the Dose Probe was approximately 1 compared to Piranha 657. The ratios did not fluctuate when the tube voltage was increased or decreased (a). The relative error was <5% when using the Dose Probe. In contrast, the relative error of the Piranha 657 was 40% (b).

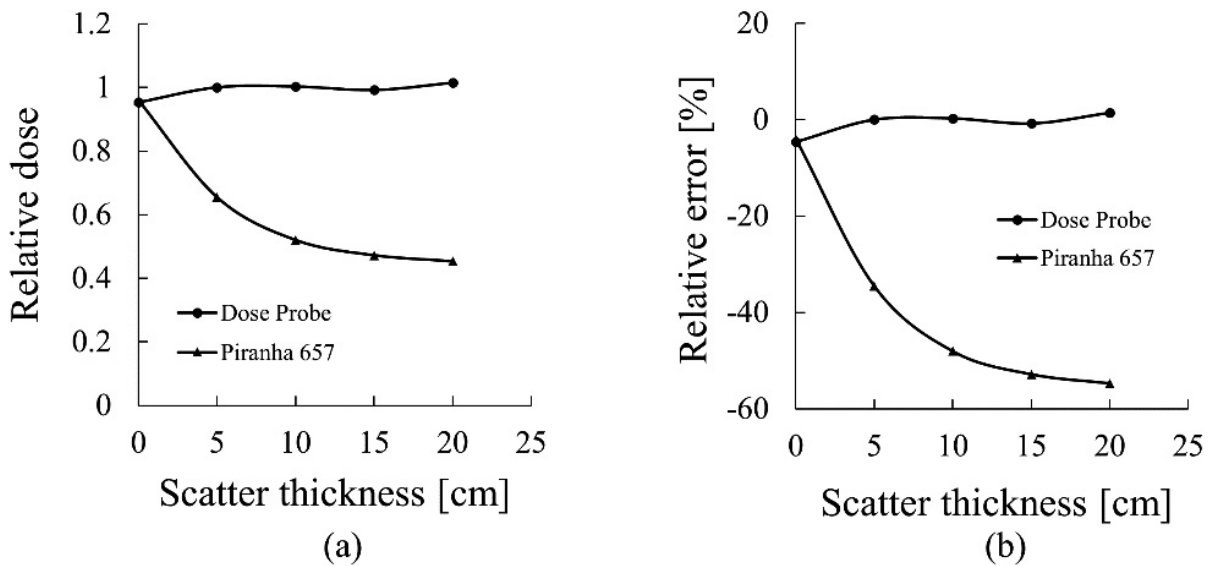


Figure 5. Ratio of the value of each semiconductor dosimeters with the value of the ion chamber at object thickness dependence.

The ratio in the case of using the Dose Probe was approximately 1 compared to Piranha 657. When the Piranha 657 was used, the ratio was became smaller (a). The relative error was <5% when using the Dose Probe. In contrast, the relative error of the Piranha 657 gradually increased (b).

5%. Conversely, the Piranha 657 had a relative error exceeding 40%. This difference might be attributed to the difference in detector surface size between the two semiconductor dosimeters. The detector surface size of the Dose Probe (approximately $10 \times 10 \text{ mm}^2$) differed from that of the Piranha 657 ($2 \times 2 \text{ mm}^2$), which may influence their respective radiation detection capabilities. This means that the Dose Probe has a higher sensitivity than the Piranha 657, and it is considered that the Dose Probe can detect scattered radiation more sensitively. Furthermore, the Dose Probe had a correction coefficient that compensated for the energy dependence from the relationship between the aluminum equivalence and tube voltage, and good energy dependence was obtained. Therefore, the Dose Probe may be advantageous for measuring air kerma, including the scattered radiation behind objects. Regarding the dose dependence, the relative value increased at 2 mAs because of an overshoot due to the short exposure time. Regarding the object-thickness dependence, the relative error of the Piranha 657 increased as the object thickness increased, whereas the relative error of the Dose Probe remained within 5%. This is because the Dose Probe detector body is thin, the detection surface is wide, and scattered radiation entering from various directions can be sufficiently detected, whereas the Piranha 657 has a narrow detection surface and detection area is set at 10 mm below from the surface. Therefore, the scattered radiation may not have been detected effectively.

This study presents a new challenge for measuring air kerma, including scattered radiation, using an externally connected semiconductor dosimeter as a preliminary step toward investigating the relationship between the incident dose on the detector and image quality. The advantage of the Dose Probe is that it does not require a complicated setup, unlike an ionization chamber, because the detector is compact and easy to handle. The results of this study showed that air kerma was measured with a relative error of <5% under conditions close to actual clinical situations (e.g., placing a detector in the space between the bed and the flat-panel detector), suggesting that it may be possible to study

the relationship between image quality and detector dose in more detail.

This study has some limitations. We measured the dose after it passed through a phantom, obtaining a correction coefficient that accounted for the changes in the energy spectrum, including scattered radiation, became challenging. Consequently, it is important to note that the use of an air-based correction coefficient may introduce some uncertainty, as the beam's energy spectrum changes after passing through the phantom. Moreover, the relationship between field size and the scattered radiation fraction requires further investigation. Although this method has some limitations, it provides crucial information on dose measurements under near-clinical conditions. This fundamental investigation serves as an important step toward understanding the relationship between detector dose and image quality in the presence of scattered radiation.

5. CONCLUSION

The response characteristics of the semiconductor dosimeter were verified through scattering using an ionization chamber as a reference dosimeter; the Dose Probe had a relative error of <5%. Ionization chambers may struggle to properly account for the dosimeter correction coefficient owing to the inclusion of scattered energy components. However, the characteristics of automatic beam-quality adjustment of the semiconductor dosimeter (the Dose Probe) are particularly effective for measuring air kerma, including scattered radiation behind objects, and have significant advantages.

Declaration of Competing Interest

The authors declare that they have no competing financial interests or personal relationships that may have influenced the work reported in this study.

Funding

This study did not receive any specific grants from funding agencies in the public, commercial, or nonprofit sectors.

REFERENCES

1. Asada Y., et. al. Textbook of medical dosimetry: Patient exposures and dosimetry for X-ray procedures. Jpn Soc Radiol Technol. 2012, pp18-31.
2. Hamasaki, H., Kato, T. Umezu, Y. Basic characteristics of a general-purpose semiconductor detector for diagnostic x-ray measurements. J JART (English ed.). 2019, 5, P.75-81.
3. Gilley R, David LR, Leamy B, Moloney D, Moore N, England A, et al. Establishing weight-based diagnostic reference levels for neonatal chest X-rays. Radiography. 2023, 29 (4), P.870-877.
4. Dos Reis CS, Caso M, Dolenc L, Howick K, Lemmen R, Meira A, et al. Optimization of exposure parameters using a phantom for thoracic spine radiographs in antero-posterior and lateral views. Radiography. 2023, 29 (5), P.870-877.
5. Mekis N, Bianchi T, Doyle C, Gauchat M, Geerling I, Linneman J, et al. Gridless adult cervical spine radiography and its' effect on image quality and radiation dose: A phantom study. Radiography. 2024, 30 (1), P.359-366.
6. Takaki T, Takeda K, Murakami S, Ogawa H, Ogawa M, Sakamoto M. Evaluation of the effects of subject thickness on the exposure index in digital radiography. Radio Phys Technol. 2016, 9, P.116-120.
7. Yasumatsu S, Tanaka N, Iwase K, Shimizu Y, Morishita J. Effect of X-ray beam quality on determination of exposure index. Radio Phys Technol. 2016, 9, P.109-115.
8. Brateman LF, Heintz PH. Solid - state dosimeters: a new approach for mammography measurements. Med Phys. 2015, 42 (2), P.542-557.
9. Ioka Y, Ariga E, Nishio N, Ooshima T. Accuracy estimation of non-invasive x-ray output analyzer. Nihon Hoshasen Gijutsu Gakkai Zasshi. 2013, 69 (10), P.1153-1160.
10. Salomon E, Homolka P, Csete I, Toroi P. Performance of semiconductor dosimeters with a range of radiation qualities used for mammography: A calibration laboratory study. Med Phys. 2020, 47 (3), P.1372-1378.